

Received November 9, 2020, accepted November 30, 2020, date of publication December 7, 2020, date of current version December 18, 2020.

Digital Object Identifier 10.1109/ACCESS.2020.3042995

Trap Level Characteristics and DC Breakdown Performance of Isotactic/Syndiotactic/Atactic Polypropylene Blend Insulation

ZHAOLIANG XING^{1,2}, CHONG ZHANG^{1,2}, MINGSHENG FAN^{1,3},
PENGFEI WU¹, XIN CHEN¹, AND ZHONGLEI LI^{1,3}, (Member, IEEE)

¹State Key Laboratory of Advanced Power Transmission Technology, Global Energy Interconnection Research Institute Company Ltd., Beijing 102209, China

²Global Energy Interconnection Research Institute Europe GmbH, 10623 Berlin, Germany

³School of Electrical and Information Engineering, Tianjin University, Tianjin 300072, China

Corresponding authors: Mingsheng Fan (fanmingsheng@tju.edu.cn) and Zhonglei Li (lizhonglei@tju.edu.cn)

This work was supported by the State Grid Corporation of China: Study on Application Technology of Polypropylene Material for DC Capacitor Film under Grant 5500-201958321A-0-0-00.

ABSTRACT Polypropylene (PP) material as a DC cable insulation material has great prospects as a recyclable alternative to cross-linked polyethylene. This paper aims at investigate the effect of PP blends crystallinity morphology and trap energy level distribution on DC breakdown strength. Five different ratios iPP/sPP/aPP blends samples are prepared by melt-blending method. Polarizing optical microscope (POM) experiments are conducted to characterize the crystallinity morphology of five iPP/sPP/aPP blends and isothermal surface potential decay (ISPD) methods are employed to measure the trap levels distribution in composite dielectric. The DC breakdown strength is tested by ball-plate electrodes equipment, and the result of DC breakdown experiment indicates that sPP30 exhibits the highest breakdown field strength, which is 29.2% higher than sPP0. The addition of sPP can act as a nucleus to help the crystallization behavior of iPP, and the distribution of spherulites in sPP30 is the most uniform and dense among the five iPP/sPP/aPP blends samples, which can improve the trap characteristics of polymers. The ISPD results show that the decay rate of the sPP30 sample is the slowest at 50 °C, 70 °C and 90 °C, indicating that sPP30 is more conducive to suppressing the dissipation process of carriers during the depolarization process. Moreover, sPP30 has higher deep trap density and lower shallow trap density and exhibits superior breakdown performance. It is deduced that the addition of sPP can effectively regulate the crystallinity morphology of iPP, and then effectively improve the trap energy level distribution of iPP/sPP/aPP blends, and it shows the improvement of DC breakdown performance macroscopically.

INDEX TERMS Polypropylene, cable insulation, crystallinity morphology, DC breakdown, trap characteristics.

I. INTRODUCTION

High-voltage DC (HVDC) cable transmission is a key technology for realizing large-capacity and long-distance transmission of electric energy and interconnection of regional power grids, and DC transmission cables have attracted more and more attention from domestic and foreign researchers [1]. As a traditional high-voltage cable insulation material, Cross-linked polyethylene (XLPE) has good electrical properties and heat resistance, but XLPE has the problems of low production efficiency, large energy consumption, and inability to recycle. Hence, in response to the development of HVDC transmission technology and to avoid environmental

problems, the development of an environmentally friendly dielectric with excellent insulation performance is one of the key issues that need to be resolved [2], [3].

Polypropylene (PP) is a thermoplastic material that is recyclable, inexpensive, and has great potential in replacing cross-linked polyethylene as a cable insulation material [4], [5]. Nevertheless, the traditional isotactic polypropylene (iPP) is not suitable for the practical application of DC cable insulation because of its high brittleness. At present, many scholars have published a large number of studies on polypropylene copolymers with different structures, including their mechanical properties, electrical strength, and thermodynamic properties. The new material stereoregular syndiotactic polypropylene (sPP) developed by Yoshino *et al.* by adding a metallocene catalyst has higher breakdown

The associate editor coordinating the review of this manuscript and approving it for publication was Jenny Mahoney.

strength, water tree resistance and thermodynamic performance than XLPE [6]. In addition, atactic polypropylene (aPP) as an elastomer, blending it with iPP can significantly improve the tensile strength and flexibility of blended PP [7]. Anders Thyssen *et al.* adjusted the crystallinity of PP samples by preparing iPP/aPP blends with different ratios, and proved that samples with higher crystallinity have higher charge storage stability [8]. Hosier *et al.* prepared different ratios of iPP and sPP blends, and conducted tensile tests and breakdown strength tests on them, and the results show that the flexibility of the blend with sPP and iPP content of 1:1 is very close to sPP, their mechanical modulus is high enough to meet the practical application of DC cables, and the mixing of sPP significantly improves the breakdown field strength of iPP [9].

The proportion of PP blends will affect the crystallinity morphology of the polymer, which will further affect the distribution of trap levels in the dielectric [10]–[13]. Moreover, the distribution of trap levels will have a crucial effect on the insulating properties of polymer dielectrics [14], [15]. Li *et al.* found that the boundaries of imperfect and fine spherulite have a large number of trap levels, thus the space charge distribution of PP will be significantly affected by the crystal morphology [16]. Li *et al.* found that the introduction of a small amount of nanoparticles can effectively increase the deep trap level and density, thereby improving the breakdown performance of polymer insulation dielectrics [17].

In this study, polarizing optical microscope (POM) experiments are conducted to characterize the crystallinity morphology of five iPP/sPP/aPP blends and isothermal surface potential decay (ISPD) methods are employed to measure the trap levels distribution in dielectric. The effects of iPP/sPP/aPP blends crystallinity morphology and trap energy level distribution on DC breakdown strength are investigated.

II. MATERIALS PREPARATION AND EXPERIMENTAL ARRANGEMENT

A. SAMPLE PREPARATION

Five kinds of iPP/sPP/aPP blends samples are prepared by melt-blending method, and the raw materials of iPP are purchased from Oasis Petroleum Inc., China and sPP and aPP are purchased from Borealis, Europe. Before the experiment, the iPP, sPP and aPP materials are dried at 60 °C for 10 hours to remove internal water molecules. iPP, sPP and aPP materials are blended into a 200 °C twin-roll mixer rotation for 20 min in a certain proportion to make them evenly dispersed. After that, the iPP/sPP/aPP blends should be put into a round mold with the pressure of 10 Mpa for 20 min at 200 °C. Then, iPP/sPP/aPP samples with thicknesses of 85 μm and 300 μm are acquired using molds of different thickness in hot-press process, which are used for DC breakdown and trap characteristic experiment, separately. The twin-roll mixer rotation (YZK-4, China) can ensure that the sample is well stirred, and the test specimens were prepared by hot press forming machine (DY-30, China), which can apply enough pressure to

TABLE 1. Index for five pp blend samples in this study.

Designation	aPP content	sPP content	iPP content
sPP0	5 wt%	0 wt%	95 wt%
sPP5	5 wt%	5 wt%	90 wt%
sPP15	5 wt%	15 wt%	80 wt%
sPP30	5 wt%	30 wt%	65 wt%
sPP45	5 wt%	45 wt%	50 wt%

prevent the specimen from forming bubbles. The proportions of five iPP/sPP/aPP samples are depicted in Table 1.

B. MATERIALS CHARACTERIZATION

POM (VHX-7000, KEYENCE, China) is employed to obtain the crystal morphology of five iPP/sPP/aPP blends. The specific operation process is as follows. First of all, a film of sample about 30 μm is pressed with a vulcanizing tablet machine, and a small piece of 2 mm diameter is cut out with clean scissors and placed in the middle of a glass slide, covered with a cover glass. The temperature was raised to 205 °C and held for 5 min to eliminate the thermal history. Then the sample is cooled to room temperature and the cooling rate is the same as that of the sample preparation, and finally the image of the sample after crystallization is obtained.

The mechanical properties of five iPP/sPP/aPP blends are characterized by the tensile strength and elongation at break. First, dumbbell shaped specimen is used for the mechanical tests, with the length, thickness and width of 30 mm, 1 mm and 4 mm, separately. Then the tensile test is conducted at 25 °C and the stretching rate is 250 mm/min.

C. DC BREAKDOWN STRENGTH

The DC breakdown strength is tested by ball-plate electrodes method in transformer oil at 30 °C to prevent air discharge and flashover. The material of the electrode is aluminum, and the diameter of the ball electrode is 25mm. The sample of 85 μm thickness is placed between the ball electrode and the plate electrode at a boost rate of 500 V/s until the sample is broken down. Each specimen is repeatedly measured 15 times.

D. ISOTHERMAL SURFACE POTENTIAL DECAY TEST

The ISPD test is conducted to calculate the trap levels distribution of iPP/sPP/aPP blends [18]–[20]. The schematic diagram of the ISPD experiment is shown in Figure 1 [21]. The vertical distance from the grid electrode to the sample surface is 5 mm. The purpose of the grid electrode is to form a parallel electric field to charge the sample and to ensure that the surface potential of the sample is equal. The distance between the needle electrode and the sample is set to about 5 mm and the needle electrode is connected to a positive direct-current source, and the voltage is set to 8 kV and applied for 8 min for corona charging. The relative humidity during the experiment is controlled at about 25% and the temperature is about at 60 °C. After charging the sample using the needle electrode, the sample is quickly moved to the Kelvin probe connected to an electrostatic voltmeter (TREK P0865, China) and measured for 1800 s, and the distance between Kelvin probe and sample is about 3 mm. Double exponential

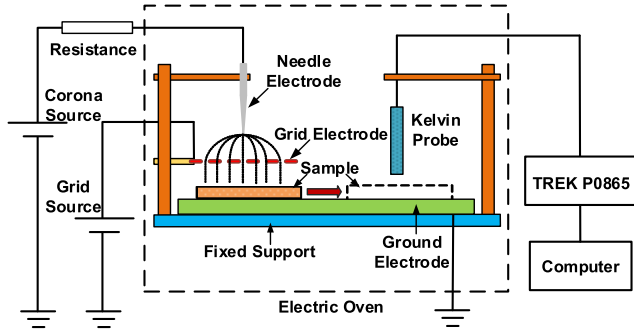


FIGURE 1. Schematic diagram of the ISPD experiment.

function can fit the surface potential attenuation curve well, which can be expressed as:

$$V_s(t) = A_1 e^{-t/\tau_1} + A_2 e^{-t/\tau_2} \quad (1)$$

where $V_s(t)$ represents the surface potential at the time t . A_1 , A_2 , τ_1 , τ_2 are the fitting parameters.

In addition, the trap energy level E_t and trap density $N_t(E_t)$ can be calculated by the following equations [22], [23]:

$$E_t = k_B T \ln(v_{ate} t) \quad (2)$$

$$N_t(E_t) = \frac{4\epsilon_0 \epsilon_r}{qL^2 k_B T} \left| t \frac{dV_s(t)}{dt} \right| \quad (3)$$

where k_B is the Boltzmann constant, and its value is 1.38×10^{-23} J/K; T is absolute temperature; v_{ate} represents escape frequency of trapped charges, which is selected as 10^{12}s^{-1} ; L is thickness of sample; ϵ_0 is vacuum permittivity and $\epsilon_r = 2.18$ is relative permittivity of PP; q is electronic charge quantity.

III. RESULTS AND DISCUSSION

A. CHARACTERIZATION OF CRYSTALLINITY MORPHOLOGY AND MECHANICAL PROPERTIES

Figure 2 presents the crystalline morphology of the five iPP/sPP/aPP blends, the crystallinity of the sample is more dense and perfect with the sPP content from 0 wt% to 30 wt%, and the diameter of their spherulites is about $25 \mu\text{m}$, but when the sPP content reaches 45 wt%, the size of spherulites in sPP45 reached close to $40 \mu\text{m}$, and large size spherulites are not uniformly distributed. The crystal morphology of sPP0 is loose, and the distance between spherulites is large. The addition of sPP can act as a nucleus to help the crystallization behavior of iPP, and the distribution of spherulites in sPP30 is the most uniform and dense among the five samples.

The elongation at break and tensile strength results of iPP/sPP/aPP blends are shown in Figure 3. It can be clearly seen that sPP0 has the highest tensile strength. With a lower (5 wt%) and higher (30 wt%) content of sPP, the elongation at break performance of iPP/sPP/aPP blends are increased compared to the sPP0.

B. ISPD RESULTS OF PP BLENDS INSULATION

Figure 4 depicts the surface potential attenuation curves after normalization of iPP/sPP/aPP blends at 50, 70 and 90 °C. The ISPD curves show an exponential decline with time,

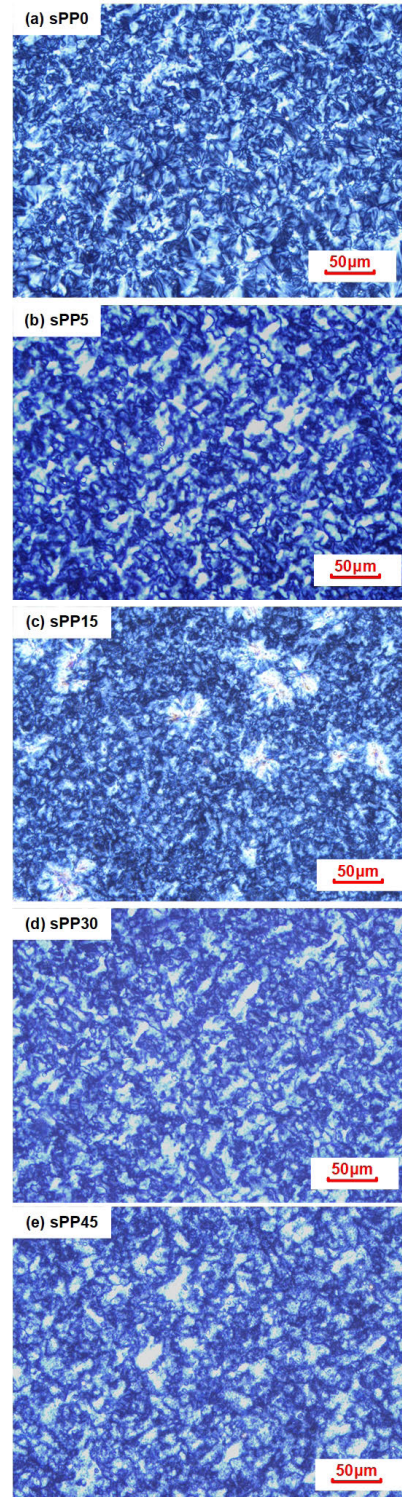


FIGURE 2. POM images of iPP/sPP/aPP blends.

and its decay rate decreases with time. During depolarization of the sample after charging, the potential of the sample surface is higher at the beginning of the attenuation, so the induced electric field formed with the back electrode is also larger, the charge in the shallow trap is prone to detrapping and migrate to the ground electrode, thus the surface potential decay rapidly. As the depolarization process proceeds, on the

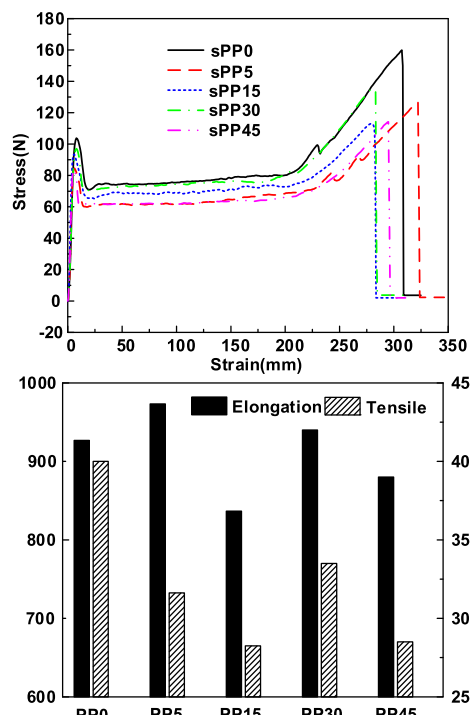


FIGURE 3. Tensile characteristics of iPP/sPP/aPP blends.

one hand, the charge in the shallow trap gradually decays and decreases, and the detrapping process of the deep trap is more difficult; on the other hand, the induced electric field formed by the surface potential and the ground electrode is getting smaller and smaller, and the charge is more difficult to detrapp, resulting in a significantly slower rate of surface potential attenuation. It can be clearly observed that as the temperature rises, the movement of the charge becomes more and more intense. More charges have enough energy to easily overcome the trap and migrate to the back electrode, so the faster the surface potential decay. At various temperatures, the decay rate of the sPP30 sample is the slowest, indicating that sPP30 is more conducive to suppressing the dissipation process of carriers during the depolarization process, thereby reducing the charge mobility and suppressing the decay of surface potential. The decay rate of sPP5, sPP15 and sPP45 potential is significantly faster than that of sPP0, which indicates that there are more shallow traps or lower energy levels of shallow traps in these samples. The imperfect spherulites in sPP5 and sPP15 and the large spherulites in sPP45 will reduce the energy level of traps and introduce a large number of shallow traps. In the process of depolarization, the charge stored in the shallow trap of the dielectric is more prone to undergo a continuous detrapping process, thus accelerating the decay rate of the surface potential.

Then the trap level distribution is calculated based on the surface potential attenuation curves, as shown in Figure 5. At 50 °C and 70 °C, the central density of the deep and shallow traps is not far from each other, and they merge into the same peak. As the temperature increases, the density of the shallow traps gradually increases and the density of the deep traps gradually decreases. The difference in the center

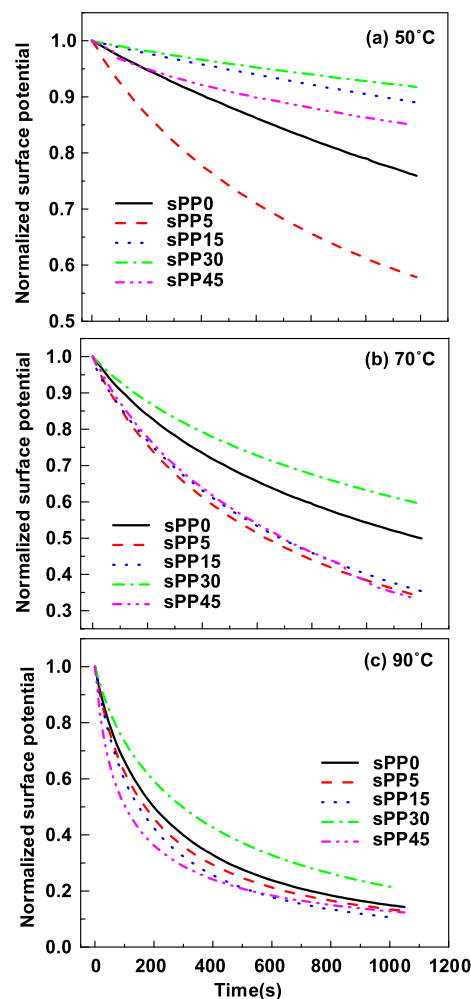


FIGURE 4. Surface potential attenuation curve after normalization of iPP/sPP/aPP blends at (a) 50 °C, (b) 70 °C and (c) 90 °C.

density of the trap gradually becomes larger, showing two different peaks. It can be seen that at 50, 70 and 90 °C, sPP30 presents the highest trap level peak. During corona charging, charge is injected into the surface of the sample and moves inside, causing the charge to accumulate on the sample. In the process of depolarization, higher temperature will trigger the detrapping process of charge carriers in deeper traps, thus accelerating the decay of surface potential [24]. At lower temperatures, most electrons do not have enough energy to transition into the conduction band, and those with enough energy are likely to scatter quickly and return to the trapped state. As the temperature increases, the energy levels of the deep and shallow traps gradually move to higher values. The charges in the deep trap are more likely to acquire activation energy at higher temperatures, so that under the action of the electro-thermal recombination field, the trapping and detrapping processes occur, causing the surface potential to decay, and finally show higher apparent trap energy level. Conversely, the activation energy provided by the electro-thermal recombination field at low temperatures can only make the carriers in the shallow trap obtain enough energy to get rid of the local state barrier, thus only a relatively shallow

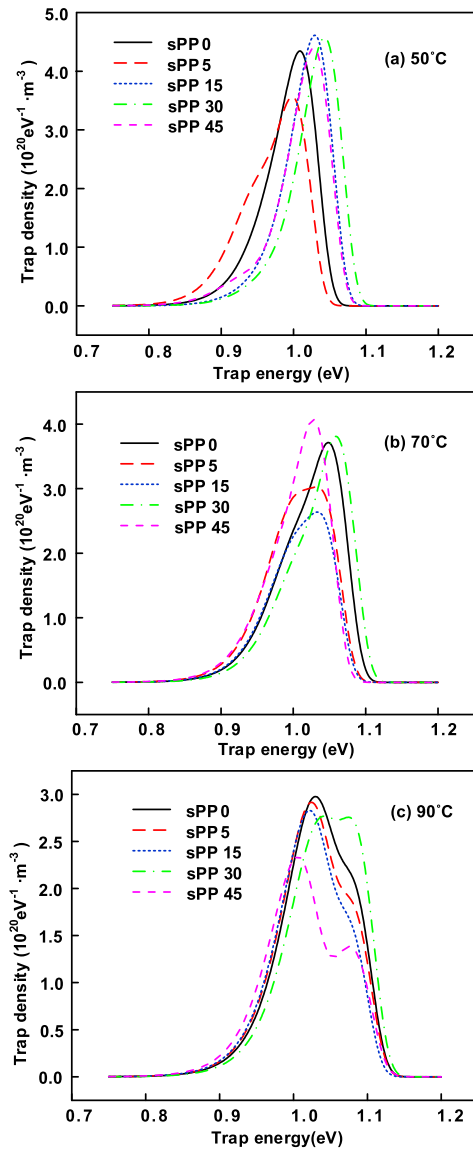


FIGURE 5. Trap level distribution of iPP/sPP/aPP blends at (a) 50 °C, (b) 70 °C and (c) 90 °C.

trap level can be exhibited. In fact, the depth of charge carrier traps in the insulation does not change with temperature, but the trap energy levels that can be measured at different temperatures are different.

C. THE PEAK SEPARATION RESULTS OF TRAP LEVEL DISTRIBUTION

In addition, the deep and shallow trap peaks are separated in this paper, that is, the A_1e^{-t/τ_1} and A_2e^{-t/τ_2} in the surface potential attenuation fitting formula (1) are separated, and the distribution curves of the deep and shallow trap energy level distribution at 50 70 and 90 °C are calculated as shown in Figures 6 and 7, respectively. The deep and shallow trap level center distributions of iPP/sPP/aPP blends at 50 °C, 70 °C and 90 °C are shown in Figure 8.

As the temperature rises, the deep and shallow trap levels of each group of samples gradually increase. For samples

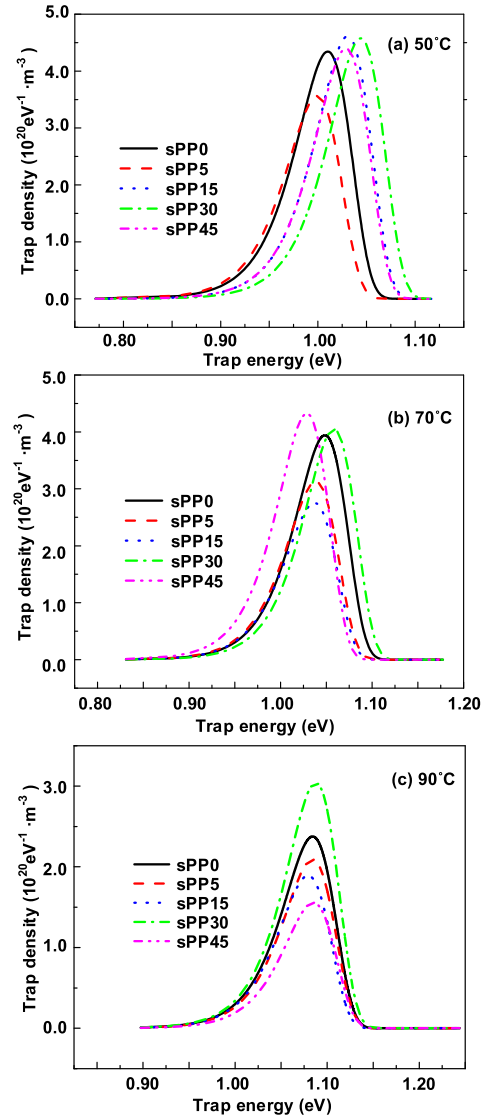


FIGURE 6. Deep trap level distribution of iPP/sPP/aPP blends at (a) 50 °C, (b) 70 °C and (c) 90 °C.

with different aPP/sPP/iPP ratios, as the mass fraction of the sPP sample increases from 0wt% to 15wt%, the energy levels of deep and shallow traps gradually decrease, except for deep trap level at 50 °C. Then, as the sPP mass fraction increases from 15wt% to 30wt%, both deep and shallow trap levels increase; furthermore, as the mass fraction of sPP increases from 30% to 45%, both deep and shallow trap levels gradually decrease. In addition, it can be found that the deep and shallow trap density centers of samples of sPP30 are almost the largest at various temperatures, and the deep trap density centers are $\sim 1.04\text{eV}$, ~ 1.06 and $\sim 1.08\text{eV}$ at 50°C, 70°C and 90°C, respectively. As a comparison, the deep trap density centers of the sPP0 samples are $\sim 1.01\text{eV}$, $\sim 1.05\text{eV}$ and $\sim 1.07\text{eV}$, respectively, indicating that the addition of an appropriate amount of sPP can introduce deeper traps in the composite dielectrics. It can also be clearly seen from the figure 8 that sPP30 has a higher level and density of deep traps and a lower density of shallow traps.

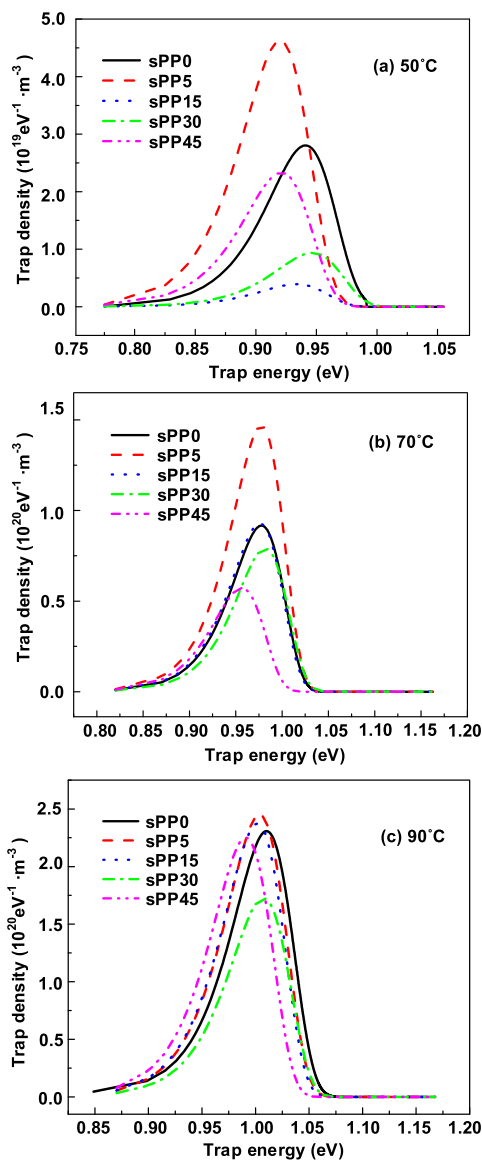


FIGURE 7. Shallow trap level distribution of iPP/sPP/aPP blends at (a) 50 °C, (b) 70 °C and (c) 90 °C.

D. BREAKDOWN PROPERTIES OF HDPE/LDPE BLENDS

DC breakdown strength results of iPP/sPP/aPP blends are shown in Figure 9. The DC breakdown strength of sPP0, sPP5, sPP15, sPP30 and sPP45 blends with Weibull distribution cumulative failure probability of 63.2% is 350.2, 281.5, 325.4, 452.3 and 417.2 kV/mm, separately. Among them, sPP30 has the highest breakdown field strength, which is 29.2% higher than sPP0.

E. EFFECTS OF CRYSTALLINE MORPHOLOGY ON TRAP CHARACTERISTICS

Blending two or more polymers can obtain better physical or chemical properties than a single polymer, so blending is an important way to obtain high-performance polymer insulation materials. PP is a semi-crystalline polymer, and its crystal morphology will have a crucial impact on the insulation performance. The addition of different proportions

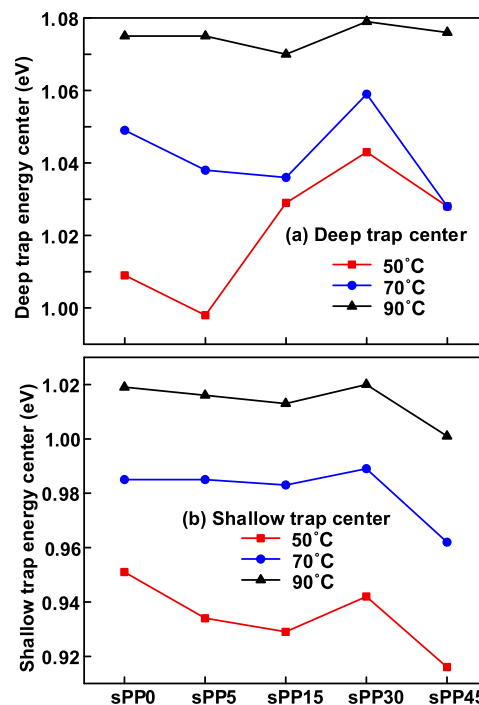


FIGURE 8. (a) Deep and (b) Shallow trap level center distribution of iPP/sPP/aPP blends at 50 °C, 70 °C and 90 °C.

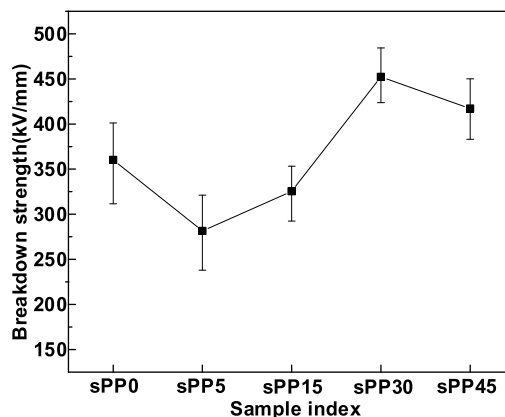


FIGURE 9. DC breakdown strength of iPP/sPP/aPP blends.

of sPP will affect the crystallization behavior of iPP, so it is necessary to pay attention to the crystallization behavior of PP blends.

The number of crystal nuclei in sPP0 is small, the growth of spherulites is large, and there are many defects between spherulites, then the charge in the polymer easily accumulates more energy under the action of the electric field through the defects, which is not conducive to polymer dielectric insulation performance. There are a lot of traps at the interface between the crystalline and amorphous regions. The addition of 30wt% sPP will introduce some impurities or groups to act as a nucleating agent, so the crystallization in PP blend will be more sufficient under the same cooling conditions. In addition, the increase in the number of crystal nuclei makes the number of spherulites in the PP blends increase and the spherulites growth is limited, thus the size of the

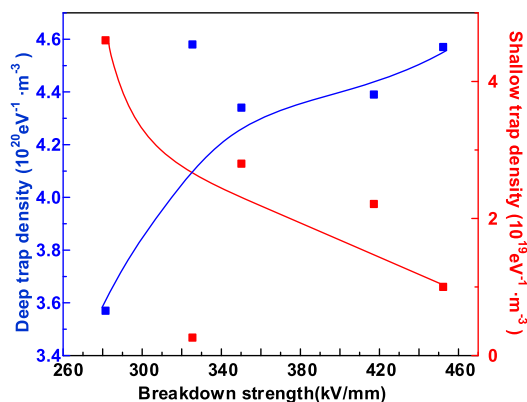


FIGURE 10. Relationship between breakdown strength and trap level characteristics measured at 50 °C of iPP/sPP/aPP blends.

spherulites decreases, so that the interface volume of the crystal region and the amorphous region becomes larger, introducing more traps improves the polymer dielectric insulation performance. Nevertheless, sPP45 contains more sPP, the size of the spherulites in the crystal morphology is larger, the arrangement between the spherulites is loose, and the interface path between the crystalline phase and the amorphous phase becomes shorter, resulting in fewer traps. Hence, the probability that charges being trapped by the trap in the dielectric will decrease due to the decrease in trap density, which is not conducive to the insulating properties of the polymer dielectric.

F. EFFECTS OF TRAP CHARACTERISTICS ON BREAKDOWN STRENGTH

Trap level and density have a crucial effect on the breakdown properties of composite dielectrics. The relationship between breakdown strength and trap level characteristics of iPP/sPP/aPP blends is shown in Figure 10. It is obvious that iPP/sPP/aPP blends can show superior breakdown characteristics when they have higher deep trap density and lower shallow trap density. The increase in the density of deep traps enhances the trapping effect and limits carrier migration, resulting in a reduction in the average free path of carriers, carrier mobility and energy, but the increase of the shallow trap density will enhance the carrier migration effect. Thus, the distribution of trap levels and density in polymer dielectrics can effectively affect the insulation properties of polymers.

IV. CONCLUSION

The addition of sPP can act as a nucleus to help the crystallization behavior of iPP, and the distribution of spherulites in sPP30 is the most uniform and dense among the five iPP/sPP/aPP blends samples. The decay rate of the sPP30 sample is the slowest at 50 °C, 70 °C and 90 °C, indicating that sPP30 is more conducive to suppressing the dissipation process of carriers during the depolarization process, thereby reducing the charge mobility and suppressing the decay of surface potential. The iPP/sPP/aPP blends samples with higher deep trap density and lower shallow trap density exhibit superior breakdown performance.

REFERENCES

- [1] G. Chen, M. Hao, Z. Xu, A. Vaughan, J. Cao, and H. Wang, "Review of high voltage direct current cables," *CSEE J. Power Energy Syst.*, vol. 1, no. 2, pp. 9–21, 2015.
- [2] Z. Li and B. Du, "Polymeric insulation for high-voltage DC extruded cables: Challenges and development directions," *IEEE Elect. Insul. Mag.*, vol. 34, no. 6, pp. 30–43, Nov. 2018.
- [3] G. Teyssedre and C. Laurent, "Advances in high-field insulating polymeric materials over the past 50 years," *IEEE Elect. Insul. Mag.*, vol. 29, no. 5, pp. 26–36, Sep. 2013.
- [4] X. Huang, Y. Fan, J. Zhang, and P. Jiang, "Polypropylene based thermoplastic polymers for potential recyclable HVDC cable insulation applications," *IEEE Trans. Dielectrics Electr. Insul.*, vol. 24, no. 3, pp. 1446–1456, Jun. 2017.
- [5] Y. Zhou, S. Peng, J. Hu, and J. He, "Polymeric insulation materials for HVDC cables: Development, challenges and future perspective," *IEEE Trans. Dielectr. Electr. Insul.*, vol. 24, no. 3, pp. 1308–1318, Jun. 2017.
- [6] K. Kurahashi, Y. Matsuda, Y. Miyashita, T. A. Demura Ueda, and K. Yoshino, "The application of novel polypropylene to the insulation of electric power cable (3)," *IEEJ Trans. Fundam. Mater.*, vol. 124, no. 4, pp. 331–336, Jan. 2004.
- [7] Z. Zhang, R. Zhang, Y. Huang, J. Lei, Y.-H. Chen, J.-H. Tang, and Z.-M. Li, "Efficient utilization of atactic polypropylene in its isotactic polypropylene blends via structuring processing," *Ind. Eng. Chem. Res.*, vol. 53, no. 24, pp. 10144–10154, Jun. 2014.
- [8] A. Thyssen, K. Almdal, and E. V. Thomsen, "Electret stability related to the crystallinity in polypropylene," *IEEE Trans. Dielectr. Electr. Insul.*, vol. 24, no. 5, pp. 3038–3046, Oct. 2017.
- [9] I. L. Hosier, A. S. Vaughan, and S. G. Swingler, "An investigation of the potential of polypropylene and its blends for use in recyclable high voltage cable insulation systems," *J. Mater. Sci.*, vol. 46, no. 11, pp. 4058–4070, Feb. 2011.
- [10] B. Dang, J. He, J. Hu, and Y. Zhou, "Large improvement in trap level and space charge distribution of polypropylene by enhancing the crystalline amorphous interface effect in blends," *Polym. Int.*, vol. 65, no. 4, pp. 371–379, Feb. 2016.
- [11] T. Yamashita and K. Ikezaki, "A method for correlating charge traps of polypropylene to its morphology," *J. Electrostatics*, vol. 63, nos. 6–10, pp. 559–564, Jun. 2005.
- [12] C. Zhang, J.-W. Zha, H.-D. Yan, W.-K. Li, and Z.-M. Dang, "High improvement in trap level density and direct current breakdown strength of block polypropylene by doping with a β -nucleating agent," *Appl. Phys. Lett.*, vol. 112, no. 9, Feb. 2018, Art. no. 091902.
- [13] Z. L. Li, B. X. Du, Z. R. Yang, and J. Li, "Effects of crystal morphology on space charge transportation and dissipation of SiC/silicone rubber composites," *IEEE Trans. Dielectr. Electr. Insul.*, vol. 24, no. 4, pp. 2616–2625, Aug. 2017.
- [14] W. Wang, D. Min, "Understanding the conduction and breakdown properties of polyethylene nanodielectrics: Effect of deep traps," *IEEE Trans. Dielectr. Electr. Insul.*, vol. 23, no. 1, pp. 72–564, Oct. 2015.
- [15] Z. Li, B. Du, C. Han, and H. Xu, "Trap modulated charge carrier transport in Polyethylene/Graphene nanocomposites," *Sci. Rep.*, vol. 7, no. 1, Jun. 2017, Art. no. 4015.
- [16] X. Li, Q. G. Du, J. Kang, and D. M. Tu, "Influence of microstructure on space charges of polypropylene," *J. Polym. Sci. B*, vol. 40, no. 4, pp. 74–365, Jan. 2002.
- [17] S. Li, D. Min, W. Wang, and G. Chen, "Linking traps to dielectric breakdown through charge dynamics for polymer nanocomposites," *IEEE Trans. Dielectr. Electr. Insul.*, vol. 23, no. 5, pp. 2777–2785, Oct. 2016.
- [18] P. Llovera and P. Molinie, "New methodology for surface potential decay measurements: Application to study charge injection dynamics on polypropylene films," *IEEE Trans. Dielectr. Electr. Insul.*, vol. 11, no. 6, pp. 1049–1056, Dec. 2004.
- [19] T. C. Zhou, G. Chen, R. J. Liao, and Z. Xu, "Charge trapping and detrapping in polymeric materials," *J. Appl. Phys.*, vol. 110, no. 4, Jan. 2011, Art. no. 043724.
- [20] Z. Li, Z. Yang, and B. Du, "Surface charge transport characteristics of ZnO/Silicone rubber composites under impulse superimposed on DC voltage," *IEEE Access*, vol. 7, pp. 3008–3017, 2019.
- [21] Z. L. Li, B. X. Du, Z. R. Yang, and C. L. Han, "Temperature dependent trap level characteristics of graphene/LDPE nanocomposites," *IEEE Trans. Dielectr. Electr. Insul.*, vol. 25, no. 1, pp. 137–144, Feb. 2018.

- [22] J. G. Simmons and M. C. Tam, "Theory of isothermal currents and the direct determination of trap parameters in semiconductors and insulators containing arbitrary trap distributions," *Phys. Rev. B, Condens. Matter*, vol. 7, no. 8, pp. 3706–3713, Apr. 1973.
- [23] J. Li, F. Zhou, D. Min, S. Li, and R. Xia, "The energy distribution of trapped charges in polymers based on isothermal surface potential decay model," *IEEE Trans. Dielectr. Electr. Insul.*, vol. 22, no. 3, pp. 1723–1732, Jun. 2015.
- [24] S. Akram, Y. Yang, X. Zhong, S. Bhutta, G. Wu, J. Castellon, and K. Zhou, "Influence of nano layer structure of polyimide film on space charge behavior and trap levels," *IEEE Trans. Dielectr. Electr. Insul.*, vol. 25, no. 4, pp. 1461–1469, Aug. 2018.



PENGFEI WU was born in Hebei, in 1986. He received the M.Sc. degree in electrical engineering from the University of Chinese Academy of Sciences. He currently works as an Engineer of insulating materials with Global Energy Interconnection Research Institute Company Ltd., for five years. His research interests include electrical materials and application technology.



ZHAOLIANG XING was born in Shandong, in 1988. He received the M.Sc. degree in high voltage and insulation technology from North China Electric Power University. He currently works as an Engineer of insulating materials with Global Energy Interconnection Research Institute Company Ltd., for six years. His research interests include polymer insulating materials and high-voltage insulation technology.



XIN CHEN was born in Neimenggu, in 1973. He received the Ph.D. degree from North China Electric Power University. He currently works as an Engineer of insulating materials with Global Energy Interconnection Research Institute Company Ltd., for 13 years. His research interests include electrical materials and application technology.



CHONG ZHANG was born in Shanxi, in 1982. He received the M.Sc. degree in materials science from Shanghai Jiaotong University. He currently works as an Engineer of insulating materials with Global Energy Interconnection Research Institute Company Ltd., for 13 years. His research interests include surface charge and space charge of polymer insulating materials.



ZHONGLEI LI (Member, IEEE) received the Ph.D. degree in electrical engineering from Tianjin University, China, in 2016. He is currently an Associate Professor with the Department of Electrical Engineering, School of Electrical and Information Engineering, Tianjin University. His research interests include dielectric property improvements and space charge of polymer insulating materials.



MINGSHENG FAN was born in Shanxi, China, in July 1997. He received the B.Sc. degree in electrical engineering from the Chengdu University of Technology, China, in 2019. He is currently pursuing the Ph.D. degree with the School of Electrical Engineering and Automation, Tianjin University. His research interests include dielectric property improvements and breakdown mechanism of polymer insulating materials.

...